Development of Diagonal Strut Mechanism of URM Wall Infilled RC Frame for Single and Double-Bays

Devjyoti PAUL[1], Ho CHOI[2], Kazuto MATSUKAWA[2], and Yoshiaki NAKANO[3]

ABSTRACT: As per the current design practice, an unreinforced masonry wall (URM) built in RC frame is considered as non-structural element. The procedure to evaluate the lateral response of a URM infilled RC frame is complex and requires high level nonlinear simulation. In this paper, a simple method to evaluate the lateral response of the URM infilled RC frame is discussed. The evaluation method is based on the 3-axis strain data measured on the concrete blocks during a static cyclic test. This strain data is used to derive an equivalent strut for every loading step. The method is tested against the results of 2 infilled RC frame specimens having single and double-bays, respectively. The calculated response showed good agreement with the test results.

Key Words: URM wall infilled RC frame, 3-axis strain measurement, Compressive diagonal strut mechanism, Equivalent strut width

INTRODUCTION

Unreinforced masonry (URM) infilled reinforced concrete (RC) frames are one of the most preferred modes of building construction around the world especially in the developing countries. The failure of URM wall infilled RC frame structures during past earthquakes has caused an extensive loss of lives. Serious research to decipher the behavior of infilled RC frames started in 1960s. However, due to the brittle nature and complex nonlinearity prevalent in URM infilled frames, the correct prediction of response of the infilled frames is not yet possible with easy analytical tools. Although a RC frame itself is ductile in nature, the infill wall changes the properties of a RC frame largely. At present the infill wall is treated as non-structural element by the design engineers, but this is not always a conservative approach. Infill walls have extremely high in-plane stiffness. When this stiffness is coupled with the RC frame's stiffness, it can drastically reduce the natural period of a building and invite higher seismic loads at the time of an earthquake than a frame assumption. However after cracking, the wall stiffness drops suddenly adding further complexity to the understanding of an infill frame behavior. Hence treating infilled walls as non-structural element is not right and it needs to be addressed well at the design stage. In this paper, a simple method to evaluate the lateral response of the URM infilled RC frame, therefore, is discussed. The evaluation method is based on the 3-axis strain data measured on the concrete blocks during a static cyclic test. This strain data is used to derive an equivalent strut for every loading step. The method is tested against the results of 2 infilled RC frame specimens having single and double-bays, respectively.

[1] Graduate student, Department of Architecture, The University of Tokyo
[2] Research Associate, Institute of Industrial Science, The University of Tokyo
[3] Director General, Professor, Institute of Industrial Science, The University of Tokyo

OVERVIEW OF REFERENCE BUILDING AND DETAILS OF SPECIMEN

Overview of Reference Building

To study the in-plane and out-of-plane behavior of URM wall infilled RC frames, an experimental program was initiated in collaboration between European and Japanese universities. A building in Turkey was chosen as reference building and 1/4 scale models were prepared in Japan for in-plane and out-of-plane test. Figure 1 shows the outline of the reference building. The reference building is a 5 storey building in Turkey, and the plan dimension is 23m by 16m. The middle frame at the first story level in the longitudinal direction is chosen for this research.

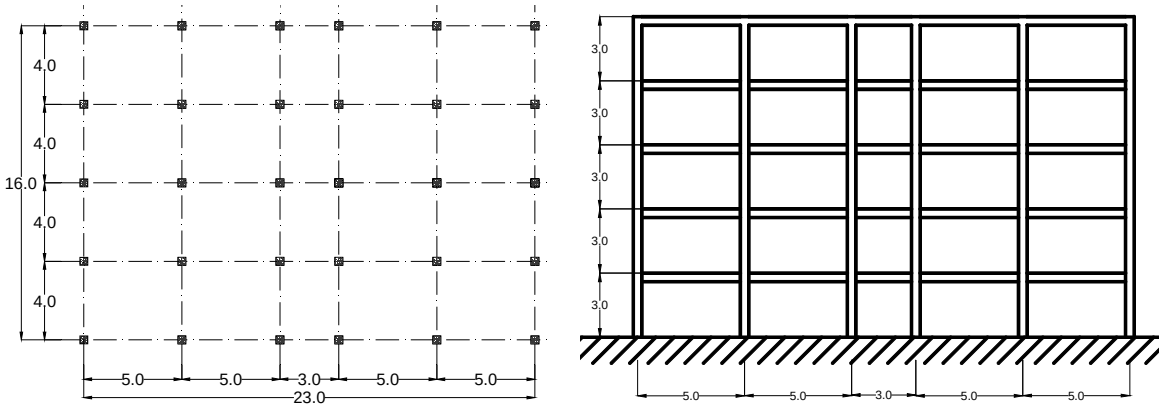

Figure 1. Outline of the Turkish Building (all dimensions are in m)

Details of Specimen

The details of the specimens are shown in Figure 2 and Figure 3. The specimens are named as Bare Frame (BF), 1-Bay 1-Storey (1B-1S), 2-Bay 1-Storey (2B-1S) specimens, respectively. The reinforcement detail of the specimen is shown in Figure 4. The size of column section is 1/4 of that of reference building. The axial stress in columns, the ratio of longitudinal reinforcement, and that of shear reinforcement are almost the same as the reference building. As shown in Figure 4, the upper beam with a T-type section, considering the effective slab width, is designed to fail in flexure, where the shear-to-flexural strength ratio (Q_{SU} / Q_{MU}) and the flexural stiffness level are both similar to those of the reference building. The concrete block (CB) unit is 1/4 of that of the full-scale unit. The cement-to-sand ratio is adjusted so that the strength and stiffness of three layered CB prism specimens should be close to those of the full-scale.

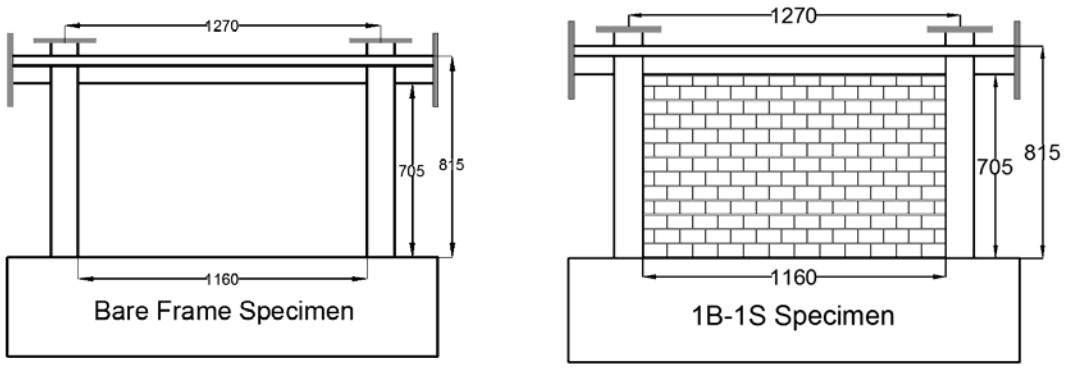

Figure 2. Details of Bare Frame and 1B-1S Specimen (all dimensions are in mm)

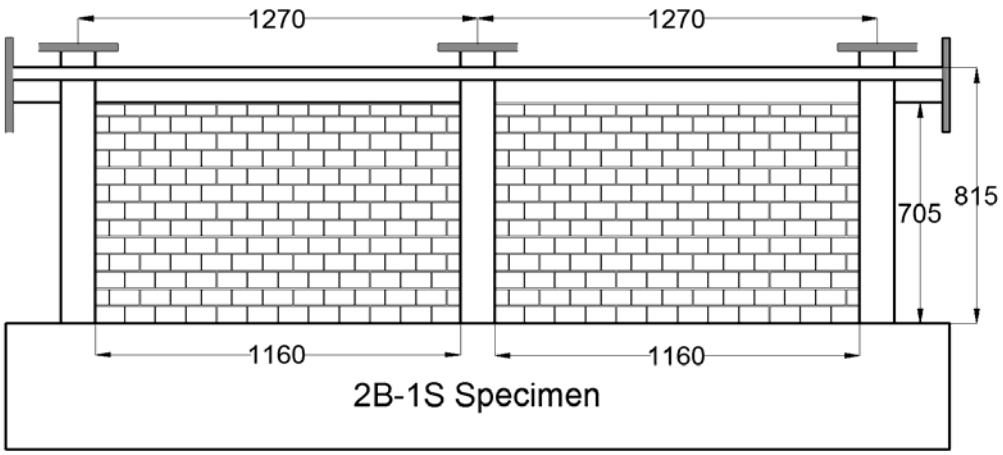

Figure 3. Details of Bare Frame and 2B-1S Specimen (all dimensions are in mm)

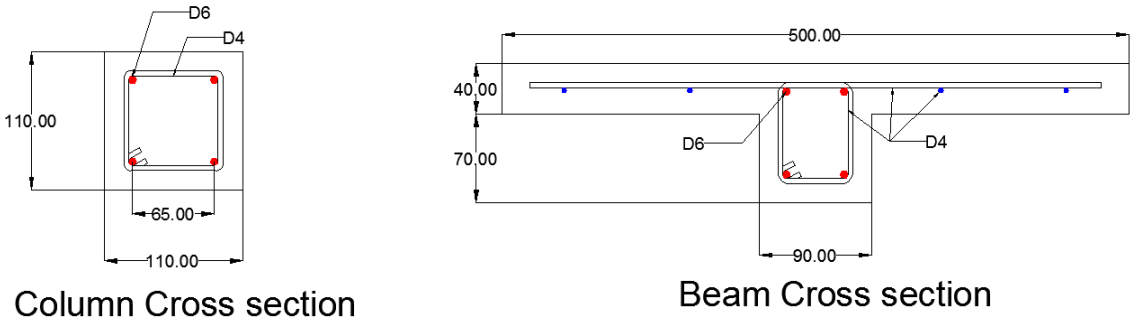

Figure 4. Cross Section Detail of Column and Beam (all dimensions are in mm)

Material Characteristic

Table 1 to Table 3 show the material test results, where the values represent the mean value of 3 samples in each test. Although the design strength of concrete is 18MPa, the compressive strength of test pieces exceeded it as shown in Table 1. The yield strength of reinforcement show higher values by 35% than the nominal strength. The compressive strength and Young's modulus from the 3 layered CB prism tests are 8.4MPa and 9.6×10^3MPa, respectively. The results obtained from the material tests were used in estimating the section capacity.

Table 1. Mechanical Properties of Concrete (Mean value of 3 samples)

Compressive strength	Elastic modulus	Split tensile strength
24.1 MPa	$2.1\text{x } 10^4$ MPa	1.71 MPa

Table 2. Mechanical Properties of Reinforcement (Mean value of 3 samples)

Bar	Use/Member	Yield strength	Tensile strength	Young's modulus
D4 Rebar (SD295)	Hoop/Beam and column	401 MPa	574 MPa	$2.1\text{x}10^5$ MPa
D6 Rebar (SD295)	Main Bar/Beam and column	407 MPa	543 MPa	$2.0\text{x}10^5$ MPa

Table 3. Mechanical Properties of Concrete Block (Mean value of 3 samples)

Compressive strength	Young's modulus
8.4 MPa	$9.6\text{x}10^3$ MPa

TEST RESULTS

Test Setup

The loading system of the specimens is shown in Figure 5. In cyclic static tests, the lateral loads were applied from the left and right end of the beam respectively with hydraulic actuators and two vertical actuators were used to apply a constant axial load of 35kN (2.9MPa) on top of each column. The loading protocol is shown in Figure 6. The displacement is measured at the center of beam. Rotation angle (R) is defined in Figure 6. The loading is done in cyclic manner in positive and negative direction.

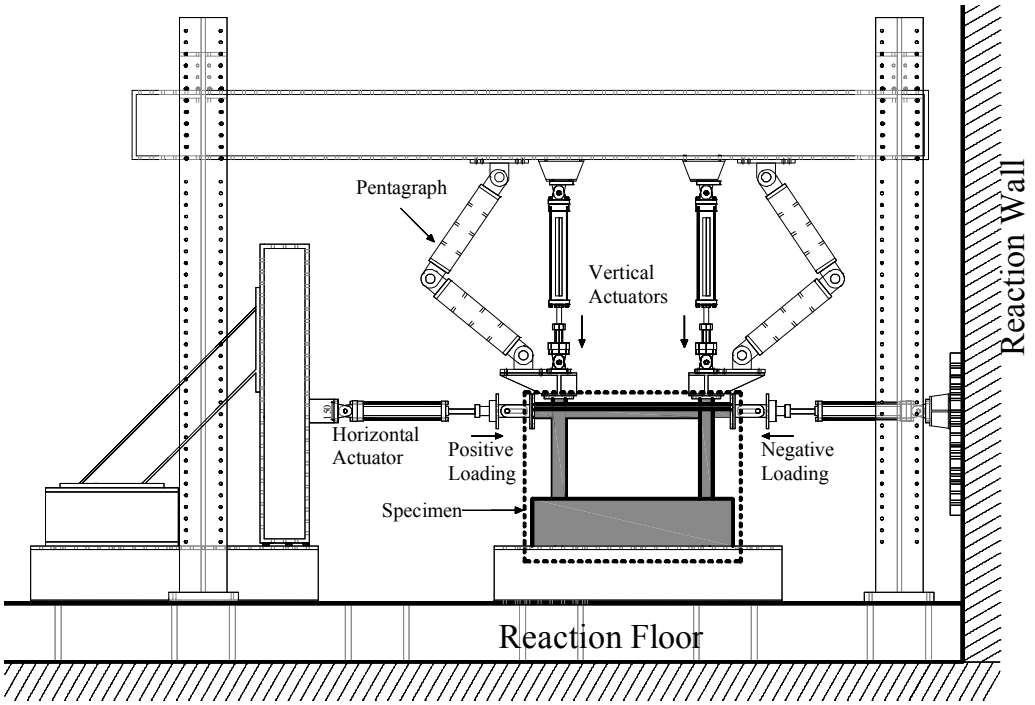

Figure 5. Test Setup

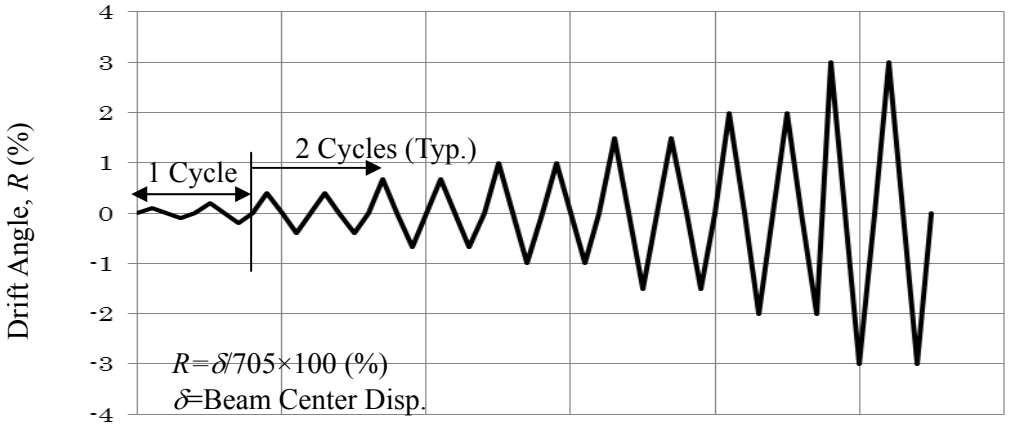

Figure 6. Loading Protocol

Failure Pattern and Load Deflection Relationships

The load deflection relationships as found during the test are shown in Figure 7 through Figure 9. The results are discussed one by one.

BF Specimen

The load deflection graph of bare frame specimen is shown in Figure 7. The First flexural crack at the bottom of tensile column appeared at +0.1% loading and the reinforcement at the bottom of tensile column yielded at +0.95%. The first shear crack appeared at the bottom of tensile column at 0.4%. The first flexural crack at top and bottom of the compression column appeared at +0.1% and 0.4% loading, respectively. The reinforcement at the bottom of the compression column yielded at +0.95%. The first shear crack appeared at the bottom of compression column at 0.67% loading. For the beam, the first flexure crack appeared near the left beam column joint at 0.25%. The reinforcement at this location yielded at +1.7%. Reinforcing bars at top side of beam, near the right beam column joint, yielded at +2.8%. The lateral load increased gradually until 1.5% loading and the maximum strength of 18.97 kN was recorded. The lateral load carrying capacity gradually deteriorated but no remarkable strength deterioration was found. The flexural crack at the left beam column joint opened rapidly from 2.5% drift angle, resulting in a flexural failure with sustained deterioration of the lateral load carrying capacity.

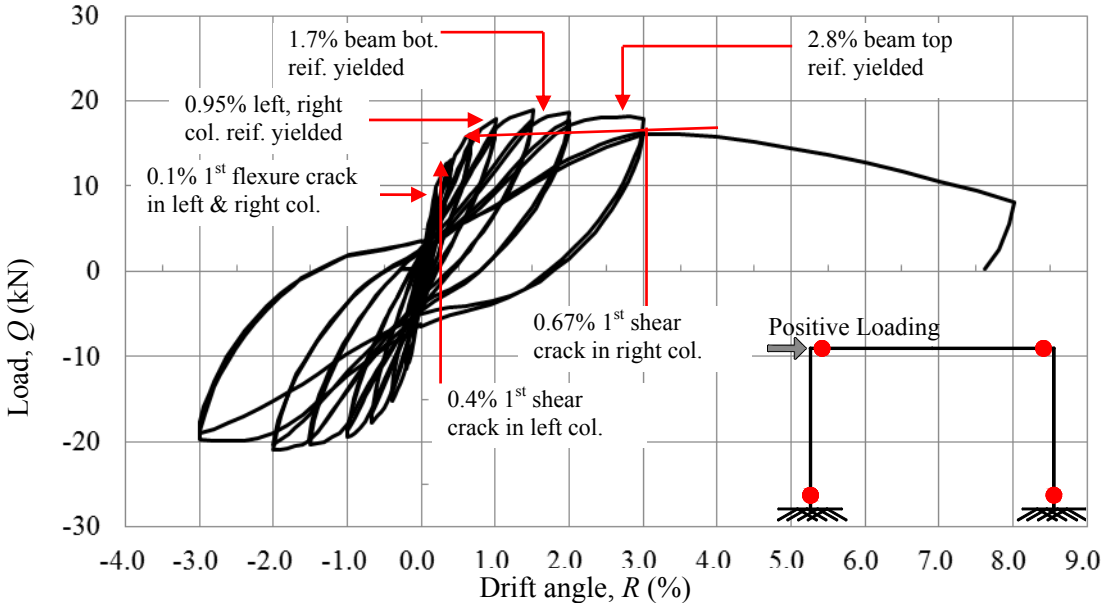

Figure 7. Test Result of BF Specimen

1B-1S Specimen

The load deflection graph of 1B-1S specimen is shown in Figure 8. The first flexural crack appeared at the top of tensile column at 0.1% loading. The flexural cracks appeared in the middle of the tensile column at +0.4% loading; this is due to short column effect arising from the presence of concrete block units.

The strain gauge data showed yielding of longitudinal reinforcement at the bottom of left column at +1.7%. However, it can be concluded from the crack pattern and calculated curvature data that the yielding of reinforcement occurred in the middle of the tensile column at around +0.67%. The first shear crack appeared at the top of tensile column at 0.4%. The first flexural crack at the bottom of the compression column appeared at 0.2% and the yielding of reinforcement at that location occurred at +1.3%. The first shear crack appeared at the bottom of compression column at 0.4%. The reinforcement at the top of compression column yielded at 2.5%.

At +0.1% loading a long bed joint crack appeared between the ninth and tenth row of blocks from the

bottom. After running through the mortar, the crack vertically propagated trough the blocks near the compression column. With increase in loading, the crack penetrated further down and the blocks above this bed-joint crack were seen to slide after 0.4% loading. At 0.4% loading, the width of this crack was 1.5mm and increased in consecutive loading cycles. The load increased until 1.0% loading, attaining a maximum load of 52.21 kN. After that the capacity of the infill frame decreased gradually.

2B-1S Specimen

The load deflection curve for the 2B-1S specimen is shown in Figure 9. The first flexural crack appeared at the top of the tensile column at +0.1% loading. The longitudinal reinforcement at the top of the tensile column yielded at +0.9%. The strain gauges at the bottom of the tensile column showed

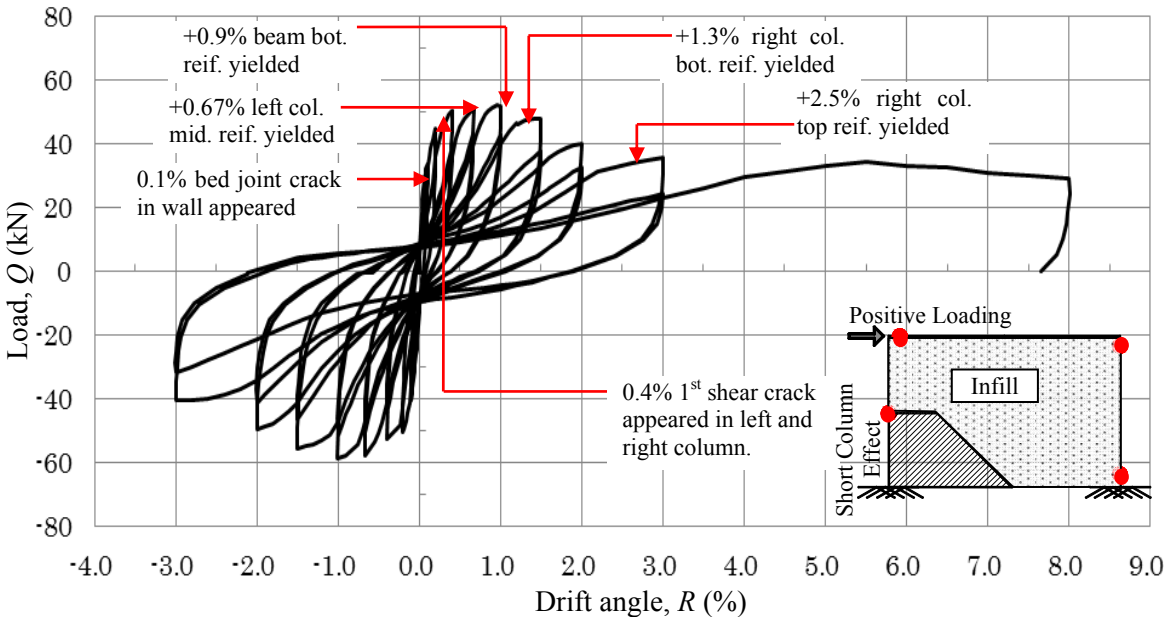

Figure 8. Test Result of 1B-1S Specimen

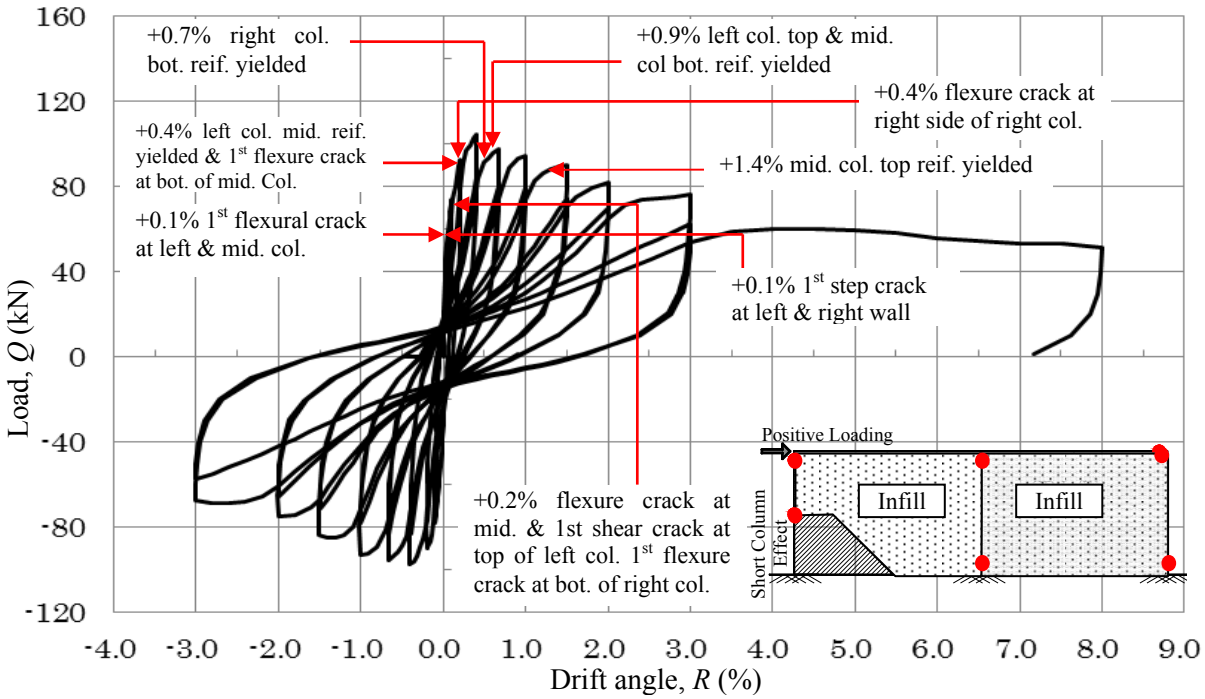

Figure 9. Test Result of 2B-1S Specimen

yielding at +1.8%. However, flexural cracks appeared in the middle of tensile column at +0.2% due to the short column effect. However, it can be concluded from the crack patterns and curvature calculation that yielding of longitudinal reinforcement in the middle of the tensile column occurred at around +0.4%. The first shear crack appeared at the top of the tensile column at 0.2% loading. For the middle column, the first flexural crack appeared at the top of column at +0.1% and the reinforcement yielded at that location at +1.4% loading. The first flexural crack appeared towards the bottom of the middle column at 0.4% and reinforcement at the bottom of middle column yielded at +0.9%. The first flexural crack at the bottom of the compression column appeared at +0.2% loading and reinforcement at this location yielded at +0.7% loading. The reinforcement at beam top near right beam column yielded at a very later stage of loading at +3.5%.

A step crack appeared in the left bay wall and propagated from left top side to right bottom side of the wall, at +0.1% loading. A similar step crack also appeared at +0.1% in the right bay wall. Both the cracks propagated until the bottom of right corner at the next loading cycle, i.e. +0.2%. As compared to the right wall, more diagonal cracks were found in the left wall for positive loading cycles and this pattern reversed for negative loading.

The load carrying capacity of the specimen increased until 0.4%. After attending the maximum value of 104.4 kN at 0.4%, the specimen showed gradual decrease in load carrying capacity over the next loading cycles. Finally the flexural cracks at the top of the tension column and middle column started to open rapidly at 2.5% loading which lead to a gradual failure of the specimen.

BRIEF EXPLANATION OF ANALYSIS PROCEDURE

The load carried by an infilled frame is basically the sum of the loads carried by the columns and the walls. The procedure to calculate the response of RC columns and infill walls are explained separately in following sections.

RC Frame Analysis Procedure

The capacity of the RC frame is basically the sum of capacities of the columns. To calculate the capacity of columns, a plastic hinge formation sequence and the effective height of the columns needs to be known. The bending moment diagram (BMD) of the columns at failure is drawn from the hinge formation sequence and the shear associated at failure is calculated from the equilibrium equations. The effect of the lateral load, applied by the horizontal actuators, is taken into consideration in calculating the axial load on the columns. The loading diagram for BF specimen is shown in Figure 10. The variable push-pull component, β arising from the application of load by horizontal actuator, is calculated at cracking and at yielding; the moment capacities of each column section is calculated from the AIJ 2010 specification for the constant axial load, N. For the sectional capacity calculation, the results obtained from material tests were used. Column curvature and BMD of BF specimen at R=1.0% is shown in Figure 11, where M_{Bb} and M_{Bt} are the sectional capacities of the beam, for positive and negative moments, respectively; M_{C1} and M_{C2} are the sectional capacities of the tension and compression column, respectively. The effect of axial force was neglected in calculating the sectional capacities of beam i.e. M_{Bb} and M_{Bt}. The difference between M_{C1} and M_{C2} is attributed to the difference in the axial stress level in the columns.

The procedure as described is used to calculate the lateral capacity of the columns. The calculation results are plotted against the test results of Bare Frame specimen in Figure 12 and it shows good agreement with the observed values during test. The same procedure is applied for the calculation of column capacity for other specimens as well.

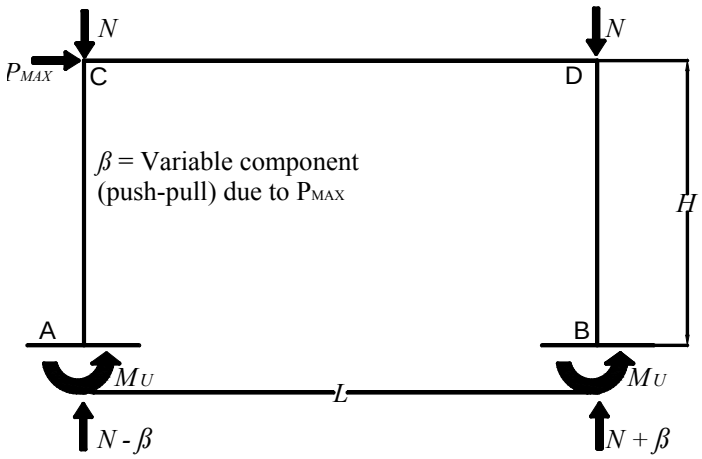

$$\beta = \frac{P_{max}H - 2M_u}{L}$$

(From equilibrium of moments at A)
M_U= Column Moment Capacity Under Constant Axial Load (N)

Figure 10. Loading Diagram of BF Specimen

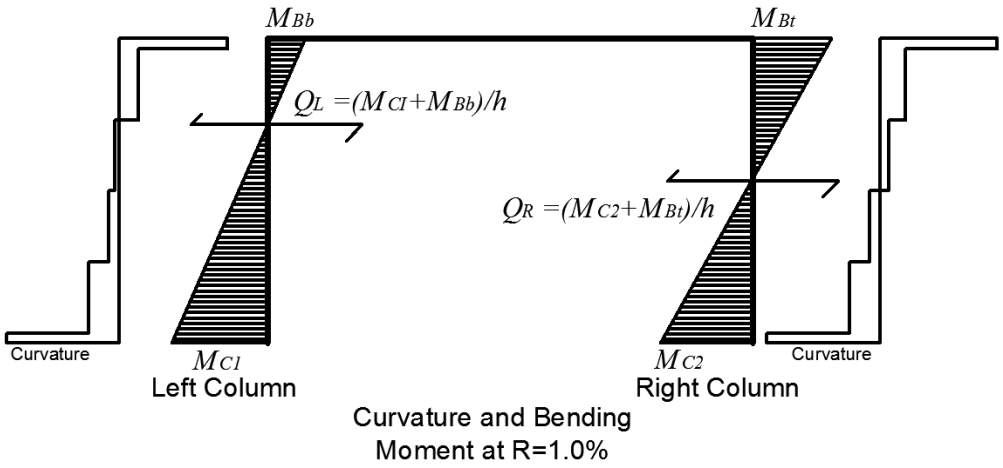

Figure 11. Bending Moment Diagram of BF Specimen

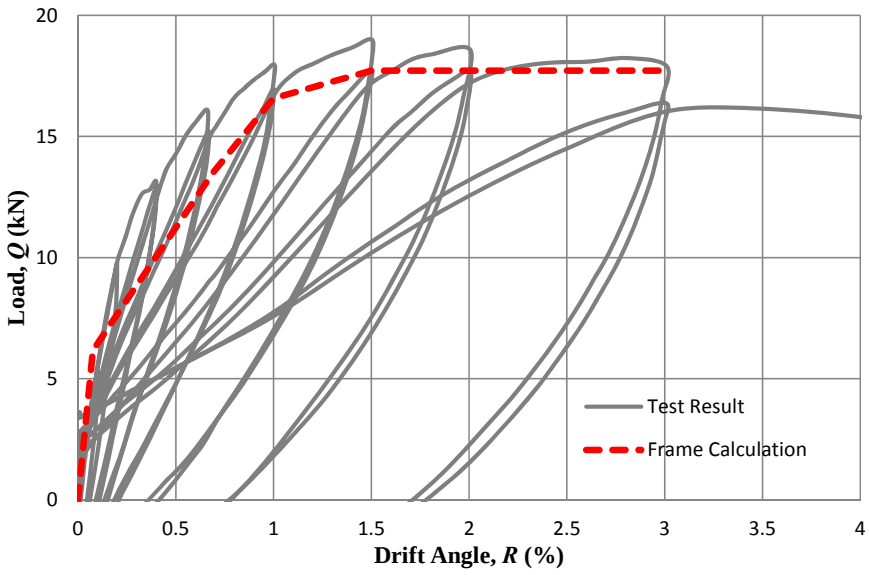

Figure 12. Comparison of Test Result & Calculation Result of Bare Frame Specimen

Wall Analysis Procedure

Wall analysis is made as per the procedure described by K. Jin 2015[1]. The procedure is described here briefly. For the analysis of the wall, the principal compressive strain and its angle are calculated from the test result at every loading step. In this procedure, the infill wall is replaced by an equivalent strut and the lateral capacity of the wall is calculated from the properties of this equivalent strut. Four main properties are needed to define the equivalent strut completely; they are the main strut angle (θ), the mean strain (ε_m) in the strut, equivalent width (W_{eq}) of the strut, and distance of the center line (C_y) of the strut from a reference point. These parameters are shown in Figure 13. Calculations of the parameters are covered in the following sub-sections and the equivalent diagonal strut model is described in Figure 15.

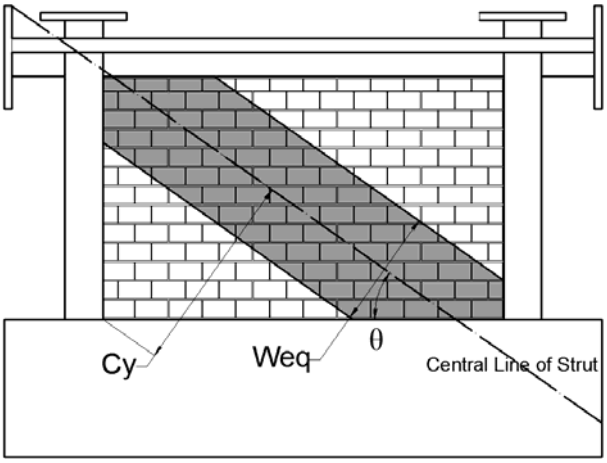

Figure 13. Description of Parameters of Equivalent Strut

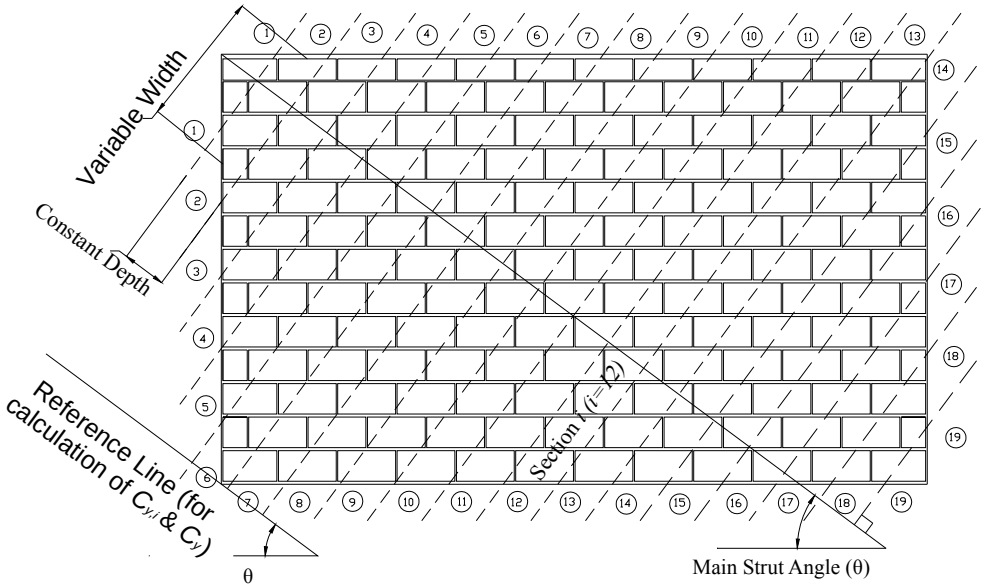

Figure 14. Section Division of Original Strut

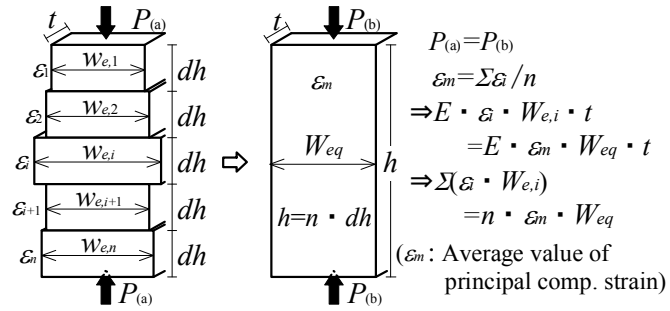

(a)Original strut (b)Equivalent strut

Figure 15. Equivalent Strut Model Parameters [1]

(1) Main strut angle (θ):

Firstly the main strut angle *(θ)* is calculated by Equation (1). All the blocks with the principle strain angle between 0 and 90 ($0<\theta j<90$) degrees is considered in this calculation, where l= number of blocks with $0<\theta j<90$, ε_j= principal compressive strain for a block, θ_j= Principal compressive strain angle of a block.

$$\theta = \left(\sum_{j=1}^{l} \varepsilon_j \times \theta_j \right) / \sum_{j=1}^{l} \varepsilon_j \qquad 0<\theta_j<90 \tag{1}$$

(2) Division of wall in sections:

To calculate the rest of the three parameters of the equivalent strut, the wall needs to be divided in a number of sections. As shown in Figure 14, a reference line with an angle θ from the horizontal axis is drawn, and equally spaced lines perpendicular to the reference are made from the lower left. The number of lines is chosen so that each section between two adjacent lines should contain at least one CB unit of each horizontal layer. The wall is divided in 19 sections at an equal interval in the diagonal direction as shown in Figure 14. The wall can be imagined as a strut with variable width. This strut with variable width is to be replaced by an equivalent strut with constant width. A same force being carried by the both struts is the main underlying assumption in calculating the equivalent strut. The equivalent strut is shown in Figure 15.

(3) Mean strain (ε_m) in the strut:

The mean value of principal compressive strain ε_i of CB units included in a section *i (i=1 to 19)* is calculated. All the blocks, with principal strain angle between 0 and 90 degrees, in section *i*, are considered in this calculation. After calculating ε_i, the mean strain in the strut (ε_m) is calculated by Equation (2).

The mean strain (ε_m) of the equivalent strut is defined as the mean of the sectional mean strains (ε_i).

$$\varepsilon_m = \sum_{i=1}^{n} \varepsilon_i / n \text{ , } (n\text{= 19 herein}) \tag{2}$$

(4) Central axis distance (C_y) for equivalent strut:

The distance of centroid ($C_{y,i}$) of CB units in a section *i (i=1 to 19)* is calculated by Equation (3), where y_i = distance of each block with $0<\theta_j<90$ at section *i* from a reference line (shown in Figure 14) , and *m*=number of blocks with $0<\theta_j<90$.

$$C_{y,i} = \left(\sum_{i=1}^{m} \varepsilon_j \times y_j \right) / \sum_{i=1}^{m} \varepsilon_j \tag{3}$$

After calculating $C_{y,i}$ for every section, the central axis distance of the equivalent strut is calculated by Equation (4).

$$C_y = \left(\sum_{i=1}^{n} \varepsilon_i \times C_{y,i} \right) / \sum_{i=1}^{n} \varepsilon_i \quad (n=19) \tag{4}$$

(5) Equivalent strut width (W_{eq}):

The effective width of strut at every section *i (i=1 to 19)* is calculated. The effective width at every section *($W_{e,i}$)* is defined as the outermost distance between the CB units having principal strain angle between 0 and 90 degrees. Please refer Figure 16 for the definition of $W_{e,i}$.

After calculating $W_{e,i}$ at every section *i* the width of the equivalent strut is calculated by Equation (5).

$$W_{eq} = \left(\sum_{i=1}^{n} (\varepsilon_i \times W_{e,i}) \right) / \sum_{i=1}^{n} \varepsilon_i \quad (n=19) \tag{5}$$

(6) Wall shear calculation:

After calculating all the parameters of the equivalent strut, the wall shear is calculated by Equation (6), where σ_m is the stress obtained from prism test of the concrete blocks corresponding to ε_m calculated for each drift angle *R*.

$$V_{CS} = W_{eq} \cdot t \cdot \sigma_m \cdot \cos\theta \tag{6}$$

The equivalent diagonal strut is calculated for every drift angle *R,* and the load deflection graph of the wall is plotted by using Equation (6).

This procedure is followed for the analysis of infill wall specimens.

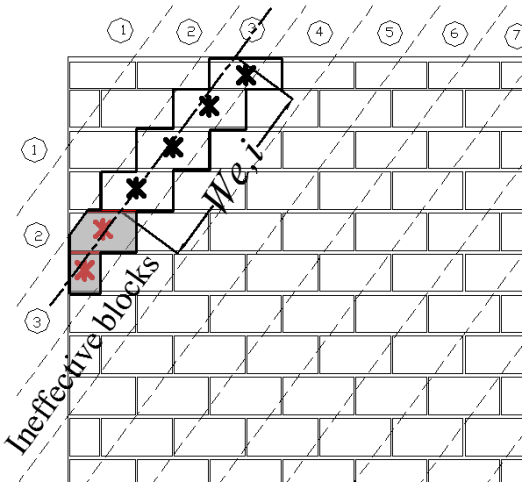

Figure 16. Width of a Section at Section *i*

STRENGTH EVALUATION RESULTS

The results of the analysis are discussed one by one.

1B-1S Specimen

The response of RC columns and infill wall is calculated separately, as described in the previous sections and added together to get the response of infill frame. The result thus obtained is plotted in Figure 17. All the blocks were taken into consideration in calculation of strut mechanism and the result is plotted in dotted line with ♦ in Figure 17. The calculated response shows good agreement with the test result until *R* = 0.4% but after that it overestimates the wall shear capacity.

As explained before, a bed joint crack separates the wall into two parts (please refer Figure 18). Studying the pictures taken during tests clearly shows that the blocks above and right side of this crack slides over brick row No. 9 (from bottom). It appeared that only the blocks under this bed crack is taking part in resisting the load after R=0.4%. This phenomenon is also clear from the plot of principal strain diagrams. As highlighted in Figure 18, the principal strain angle of the blocks above and below the crack became almost flat at 0.4% loading. From these observations, another trial of calculation was made, considering only the blocks below this crack from R=0.67%. As sliding is a rigid body motion, the blocks undergoing sliding were excluded in diagonal strut calculation. Figure 19 shows the blocks

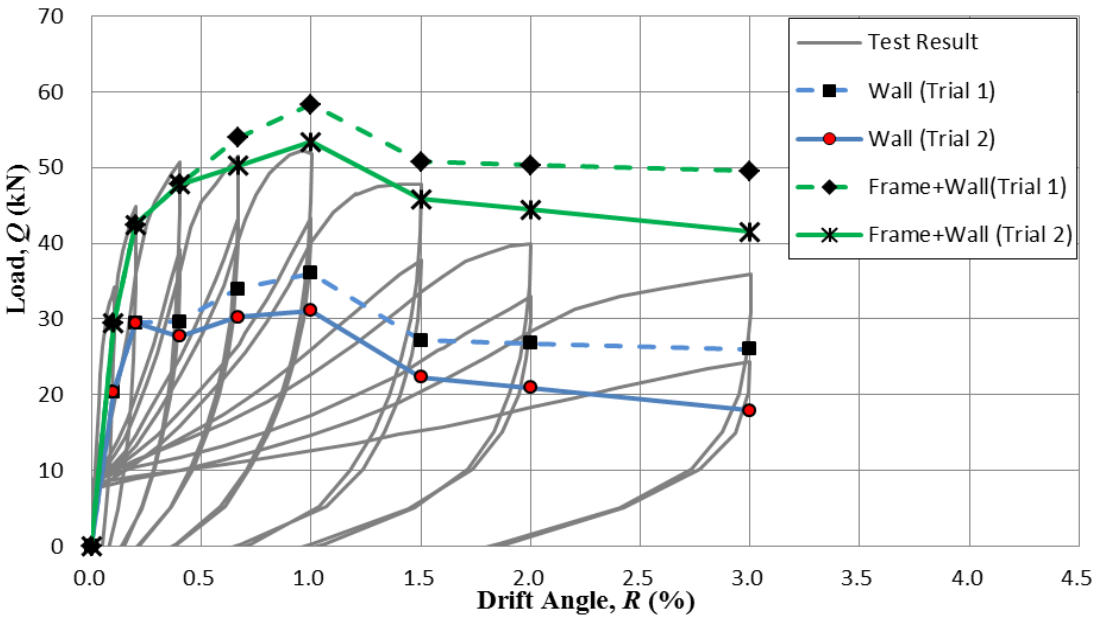

Figure 17. Load Deflection Curve for 1B-1S Specimen

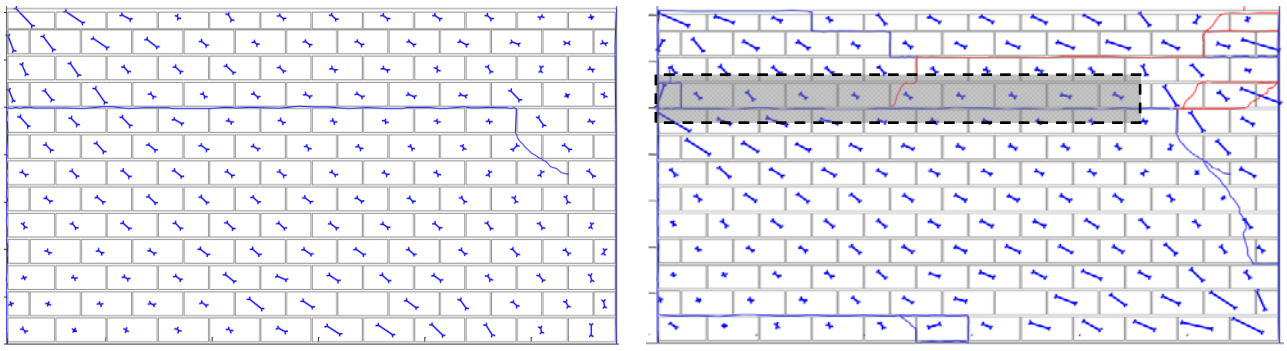

R=0.1% R=0.4%

Figure 18. Principal Strain Distribution at R=0.1% and R=0.4%

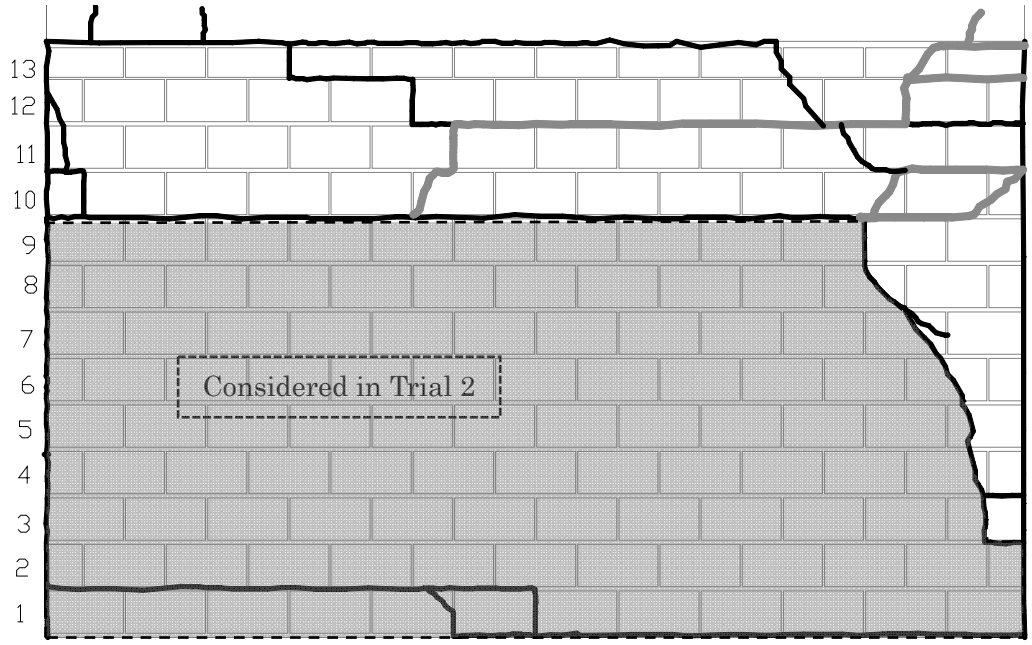

Black Line Denotes the Cracks Generated by Positive Loading
Gray Line Denotes the Cracks Generated by Negative Loading

Figure 19. Crack pattern at R=0.67% 1B-1S Specimen

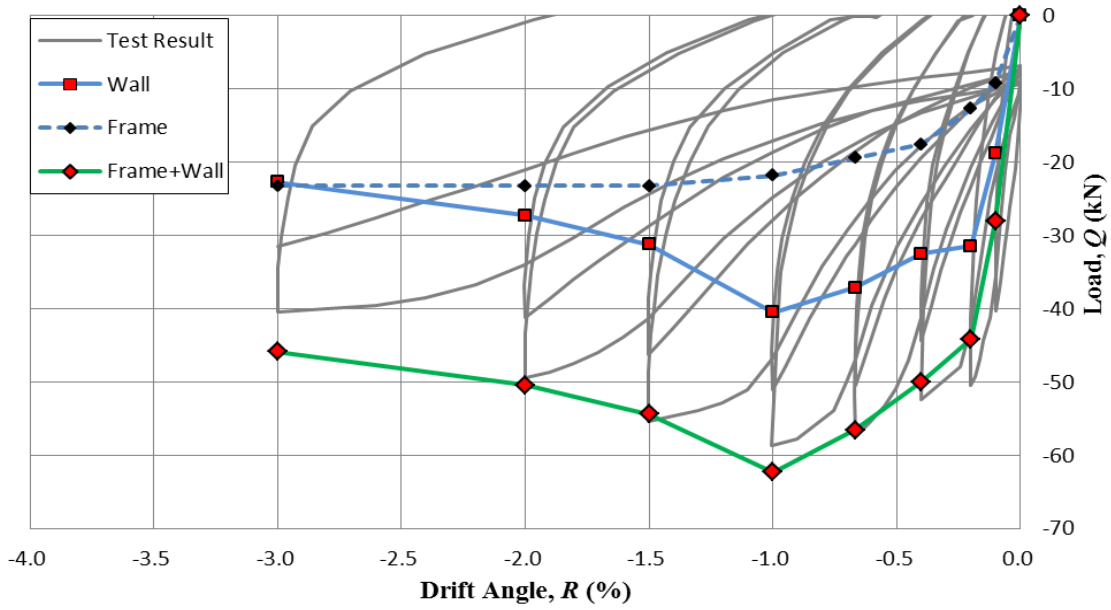

Figure 20. Load Deflection Curve for 1B-1S Specimen for Negative Direction

selected for the 2nd trial, shown in hatched. The result of this second trial is presented in solid line with * in Figure 17. It shows much better agreement with the test results throughout the loading cycle.
The response of the specimen was also calculated in the negative direction of loading. The results are shown in Figure 20. The result shows good agreement with the test result throughout the loading cycles.

2B-1S Specimen

The same procedure is followed to calculate the response of 2B-1S specimen. However, due to limitations in the measurement equipment, it was not possible to measure 3-axis strain data for all the blocks. Certain blocks were therefore, selected to measure the strain. Selection of blocks was made to evaluate the strut mechanism in the positive loading direction. Please refer to Figure 21 for the arrangement of blocks with strain gauges.

As the number of strain gauge data on block is half as compared to 1B-1S specimen, the method used for wall analysis of 1B-1S specimen needs to be modified.

It is assumed that every strain data point now represents the strain condition of an area larger than a single block. The influence zone of a data point represented by the measured data is defined in Figure 22. If a data point shows that the value of the principal strain angle is not between 0 and 90 degrees, then the area represented by the data point is considered as ineffective in strut action. In calculation of effective strut width at a section $(W_{e,i})$ for 2B-1S specimen, the same logic is followed and the ineffective area to be excluded is shown in Figure 22.

Verification of the Proposed Modification

To check the suitability of this assumption in data, the 1B-1S specimen is re-calculated with reduced number of gauges. Gauges located exactly at the same location as the 2-bay specimen are chosen for this purpose. The result thus obtained is compared with the result obtained previously using data from all the blocks. This analysis is made for the negative loading cycle of the 1B-1S specimen. The results obtained are shown in Figure 23.

A good agreement is confirmed between the results obtained from half of the blocks and using all the blocks. Hence, the modified method can be applied for calculating the response of the 2B-1S specimen as well.

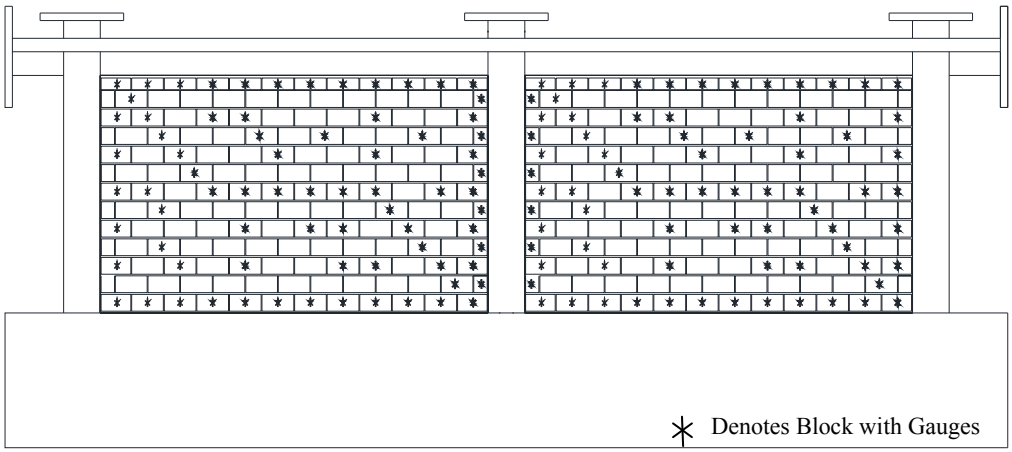

Figure 21. Strain Gauge Pattern in 2-Bay Specimen

Analysis Result of 2B-1S Specimen

Frame calculation for 2B-1S specimen was done in a similar way to Bare Frame and 1B-1S specimens. Wall analysis procedure was modified as the data was limited. However, upon verification of the assumption in analysis method, the left and right walls are analyzed separately and added together to get the response of the specimen. The results are plotted in Figure 24.

The test results and calculated results show good agreement. However the calculated peak load is about 8% less than the observed value during the experiment.

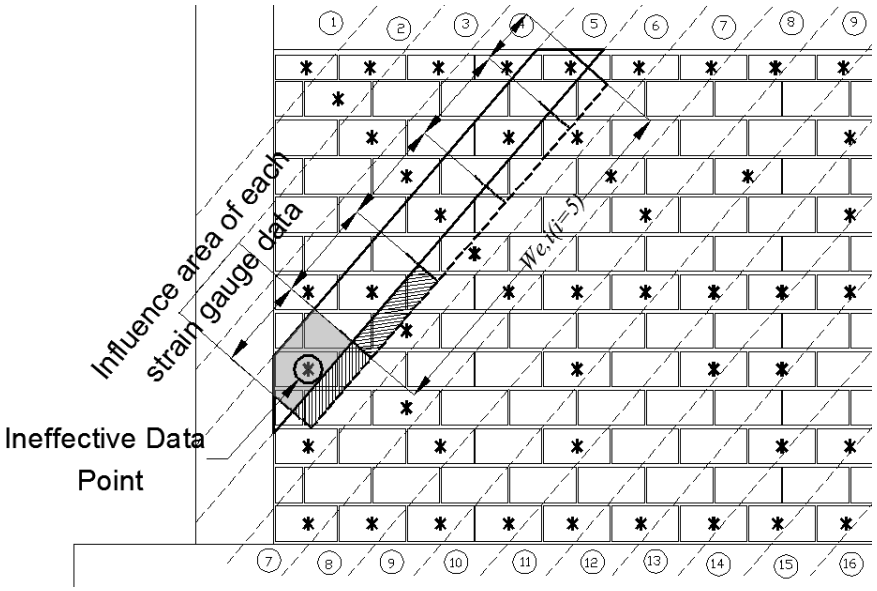

Figure 22. Influence Area of a Strain Data Measurement Point and Effective Width of Section for 2B-1S Specimen

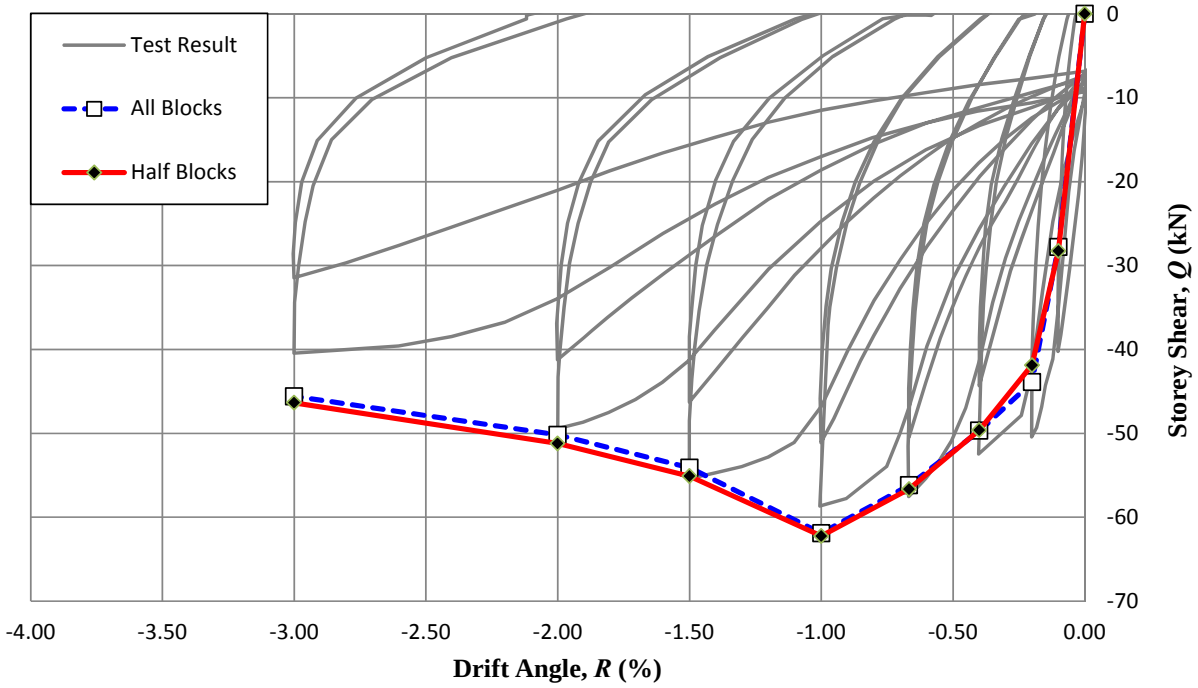

Figure 23. Comparison of All Blocks & Half Blocks Response of 1B-1S Specimen

Equivalent Strut of 1B-1S and 2B-1S Specimens

The equivalent struts computed for the calculation of the response is drawn for comparison. Equivalent strut is drawn for 1B-1S and 2B-1S specimens for the maximum response. Maximum response comes for 1B-1S specimen and 2B-1S specimen at 1.0% and 0.4% loading, respectively. Please refer to Figure 25 for 1B-1S and Figure 26 for 2B-1S specimen equivalent strut results.

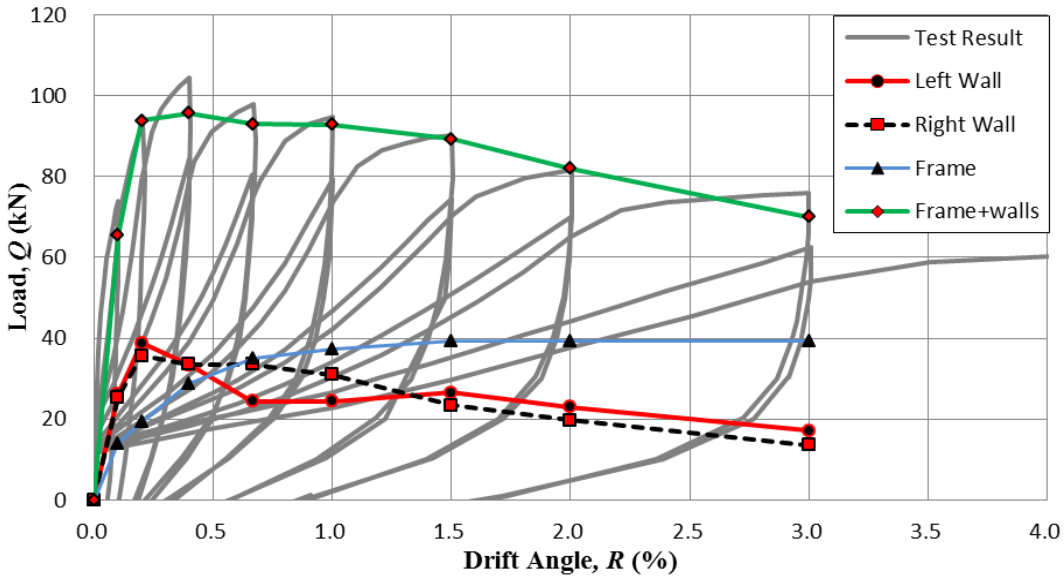

Figure 24. Load Deflection Curve of 2B-1S Specimen

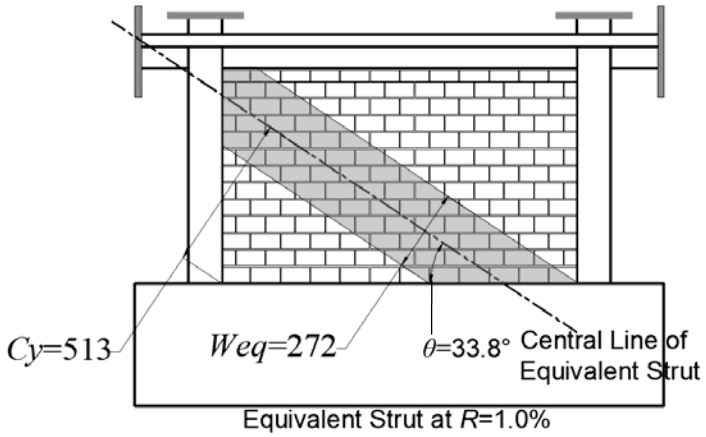

Figure 25. Equivalent Strut of 1B-1S Specimen at Maximum Response (all dimensions are in mm)

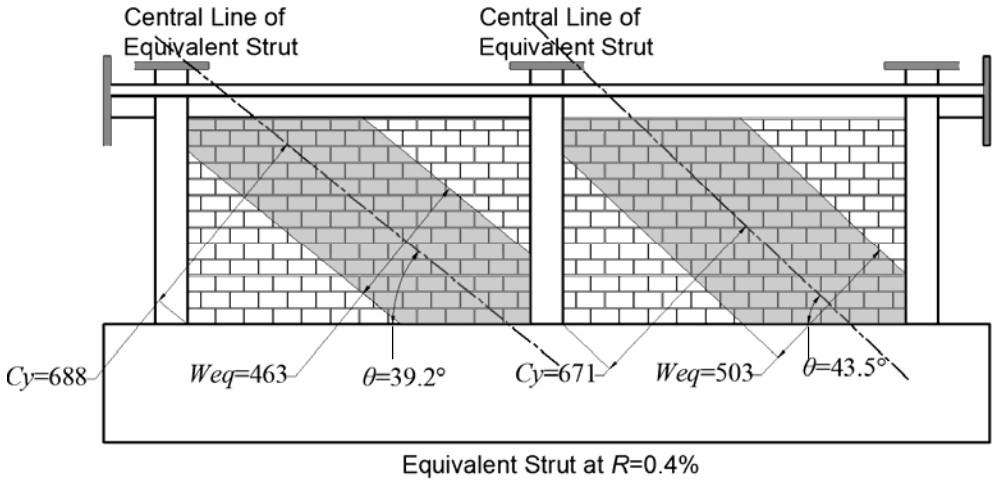

Figure 26. Equivalent strut of 2B-1S Specimen at Maximum Response (all dimensions are in mm)

CONCLUSIONS

A simplified analysis method for URM infilled RC frame is discussed and the same is verified against the test results for bare frame, 1B-1S and 2B-1S specimen. This method was applied before as well [1] but it was applied only for 1-bay 1-story specimens. From the results of this analysis, the major findings can be summarized as follows.

(1) The equivalent diagonal strut method can accurately estimate the wall response for 1 bay and 2 bay specimen throughout the loading cycle.
(2) Careful consideration needs to be given while selecting the blocks for analysis, as blocks undergoing sliding do not take part in strut formation and hence need to be excluded.
(3) It is possible to obtain accurate response of a frame even if strain data is not available for all the blocks. Careful considerations should be given in selecting the blocks for strain data measurement if all the blocks are not selected for strain measurement.

ACKNOWLEDGMENT

The project was funded by Connecting and Coordinating European Research and Technology Development with Japan (CONCERT-Japan, Project leader: Professor Polat Gulkan of Cankaya Unversity, Turkey, Project leader for Japan: Professor Yoshiaki Nakano) under Japan Science and Technology Agency. The authors are greatly thankful for the financial support.

REFERENCES

Jin, K., Choi, H., Takahashi, N., Nakano, Y. (2012). “Failure Mechanism and Seismic Capacity of RC Frames with URM Wall considering Its Diagonal Strut”. *Proc. 15th World Conference of Earthquake Engineering (WCEE), International Association of Earthquake Engineering.*

Architectural Institute of Japan (AIJ)-2010: AIJ Standard for Structural Calculation of Reinforced Concrete Structures.